

Simultaneous reconstruction of an obstacle and its wavenumber for the Helmholtz equation: a robust optimization approach

Thomas Bonnafont^{*1}, Fabien Caubet^{†2}, Nicolas Grima^{‡2}, and Jason Tridon^{§2}

¹Lab-STICC, UMR CNRS 6285, ENSTA, Institut Polytechnique de Paris, Brest, France

²Université de Pau et des Pays de l'Adour, E2S UPPA, CNRS, LMAP, UMR 5142, 64000 Pau, France.

November 18, 2025

Abstract

In this paper, we propose a method to recover simultaneously the shape and wavenumber of an object from noisy radar or sonar measurements. The physical problem is modeled in a bounded domain with the Helmholtz equation and appropriate transmission conditions. The approach relies on a Kohn–Vogelius formulation of the inverse problem and uses Nesterov's accelerated gradient descent combined with shape optimization techniques. To address the robustness of the method with respect to measurement noise, we are looking to minimize a convex combination of the expected value and variance, which we achieve by using a Karhunen–Loève expansion. The effectiveness of the approach is demonstrated through two-dimensional numerical experiments.

Keywords: inverse problems, shape optimization, Helmholtz equation, noisy data, inverse scattering problem

AMS Classification: 35R30, 35J05, 49Q10

1 Introduction

1.1 Motivations

The inverse scattering problem [10] consists in retrieving the physical and parametric properties of an object from radar or sonar measurements. This problem is of major interest in numerous applications, including defense, non-destructive testing, health monitoring, and geoscience. For a general mathematical background on this problem, we refer to the works of Colton and Kress [13, 10, 14, 8].

This work is situated within this context, with the objective of detecting and reconstructing both the shape and the wavenumber of an unknown object from radar measurements while accounting for uncertainties. We expect this strategy to overcome the problem of ill-posedness of retrieving the wavenumber alone [13, 10]. Here, as usual, we consider the case of monochromatic incident waves and thus deal with the Helmholtz equation, with Robin boundary condition. This outer boundary condition models the Sommerfeld one on a bounded domain. Finally, since we are interested in reconstructing the shape of the target and its wavenumber, the governing equations involve transmission conditions on the unknown interface between the object and the exterior environment. Our transmission condition models a situation in which the dielectric permittivity ε of the object differs from that of the surrounding medium.

^{*}thomas.bonnafont.enac@gmail.com

[†]fabien.caubet@univ-pau.fr

[‡]nicolas.grima@univ-pau.fr

[§]jason.tridon@univ-pau.fr

The adopted strategy is the minimization of an objective functional of Kohn-Vogelius type using Nesterov's accelerated gradient descent. From a numerical point of view, we parameterize the shape by a truncated Fourier series. This allows us to work naturally in a finite-dimensional space. Our methodology thus relies on tools from shape optimization, presented in the books of Allaire [2], and Henrot and Pierre [24].

Previous studies have considered the shape reconstruction for a similar problem. We can highlight the work [26] where an exterior Sommerfeld radiation condition is employed. As previously mentioned, we approximate this condition by the Robin condition. This specific choice allows us to efficiently solve the underlying equations using a finite element method. A further key difference is that they, along with many other authors (e.g., [19, 3]), employ level-set methods, that allow one to consider topological change. However, this does not address the ill-posedness of the inverse scattering problem while our parametrization addresses this issue naturally. Finally, we highlight that they do not consider the reconstruction of the wavenumber.

On the other hand, another strand of the literature consider the case of directly retrieving the dielectric parameters of the target. For instance, some relevant works include linear sampling method (see, e.g., [7, 9, 15]). Indeed, this problem has been shown to be very ill-posed and the methods are mostly based on a linearization of the integral equation in order to inverse the system and retrieve the wavenumber of the object, and in the same time its shape. Nonetheless, this method are still limited and the result highly depend on the contrast between the target and the surrounding domain.

Here, we do not consider thin-layers, but in another context, the transmission condition can be replaced by modeling it through a Ventcel-type condition [25, 6]. Various studies have investigated the simultaneous reconstruction of the thickness and the impedance condition of the unknown object as [5]. Those analysis does not incorporate data uncertainties into the reconstruction model. Also, we can remark that in [5], the authors prove the following identifiability result: the solution to the inverse problem is unique assuming that any directions of observations and scattering are known. This question, while very important, will not be considered in the present work.

The use of the Kohn-Vogelius functional has previously been considered in other physical problems, see [11, 16, 12]. Indeed, this approach has shown to be better than the conventional least-square one, even for a simple inverse scattering case where homogeneous Dirichlet condition is considered for the target boundary [4]. In particular, in [16] they introduced a Karhunen–Loëve expansion to handle uncertainties in the measurements, which we similarly employ in the present study. The authors also seek to reconstruct an object using shape optimization. However, their work is set within the framework of obstacle reconstruction with Poisson equation.

This paper is organized as follows. Section 2 presents the equations under study and the main results we obtained. We introduce a Kohn-Vogelius, which is specifically constructed so that its minimizers coincide with the solutions of the inverse problem. We prove the existence and give the expressions of the derivatives for both the deterministic case and the case with uncertainties. In the latter case, we develop the Karhunen–Loëve expansion that permits us to replace the cost functional by moments of order 1 and 2 of the deterministic Kohn-Vogelius functional. Section 3 is devoted to illustrate our method by numerical experiments. In particular, we highlight the advantages of the robust approach. In these experiments, the objects are represented by truncated Fourier expansions and we minimize the cost functional, thanks to a Nesterov descent scheme. Section 4 shows that the equations considered are well-posed and addresses the proofs of the principal results.

1.2 Notations and setting of the inverse problem

Notations. As previously mentioned, in this paper, we focus on an inverse scattering problem. In particular, even if the work is general, we use the notation of electromagnetic. The situation can be stated quite simply: we want to detect and reconstruct an unknown obstacle \mathcal{O} (which could be, for instance, a tumor or an airplane), assumed to be included in a domain \mathcal{D} , and its wavenumber, from electromagnetic measurements.

We study the harmonic case, and thus assume an $\exp(-i2\pi ft)$ -time variation where f is the frequency, inducing the $\exp(ikr)$ space variations. In all the following, \mathcal{D} denotes a bounded domain, i.e. a connected open subset of \mathbb{R}^d ($d = 2, 3$) with Lipschitz boundary. To detect the object \mathcal{O} , we send planar waves on this object and we measure a signal u_{obs} via some sensors (such as antennas) on part of the boundary of \mathcal{D} here denoted by Γ_m . The boundary Γ_c denotes the part of the boundary that is not covered by the sensors. Hence, we have $\partial\mathcal{D} = \overline{\Gamma_m \cup \Gamma_c}$. Both parts are not necessarily connected. The Robin condition is imposed on $\partial\mathcal{D}$. The wave sent corresponds to the incident wave u_{inc} and the wave that comes back to us is the sum of the scattered wave u_s and u_{inc} , that is $u = u_{\text{inc}} + u_s$. Hence, we know u_{inc} everywhere and we also know the sum $u = u_{\text{obs}} = u_{\text{inc}} + u_s$ on the sensors Γ_m . For a schematic representation of the inverse scattering problem, one can refer to Figure 1.

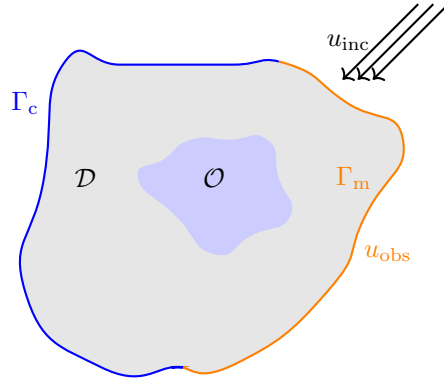


Figure 1: An example of scattering inverse problem.

In the following, we will consider the following set of admissible shapes \mathcal{O} :

$$\mathcal{U}_{\text{adm}} = \{\mathcal{O} \subset \mathcal{D}; \mathcal{O} \text{ is closed with Lipschitz boundary and such that } \mathcal{D} \setminus \mathcal{O} \text{ is connected}\}.$$

We also assume that the wavenumber is constant in both \mathcal{O} and $\mathcal{D} \setminus \mathcal{O}$. From now on, we write \mathcal{O}_1 the unknown and $\mathcal{O}_2 = \mathcal{D} \setminus \mathcal{O}_1$ such that the wavenumber on \mathcal{O}_j is written k_j , $j = 1, 2$. Notice that k_1 is then unknown and k_2 is known. In the following, we assume that

$$\Im(k_2) > 0$$

and we will consider the following set of admissible wavenumber $\mathfrak{K}_{\text{adm}}$:

$$\mathfrak{K}_{\text{adm}} = \{k_1 \in \mathbb{C}; \Re(k_1)\Re(k_2) > 0 \text{ and } \Im(k_1) > 0\}.$$

The conditions on the imaginary parts of the wavenumbers are in line with the convention we choose for the time-variation. It shall also be noted that this also ensure the condition on the real part of k_1 and k_2 since they will be of same sign. In the other case, both imaginary parts are negative provided that we also change the sign of the term $-iku$ in the Robin condition.

Setting of the inverse problem. The inverse problem can then be stated as follows: we aim to find an admissible shape $\mathcal{O}_1 \in \mathcal{U}_{\text{adm}}$, an admissible wavenumber $k_1 \in \mathfrak{K}_{\text{adm}}$ and $u \in V$ such that

$$\begin{cases} \Delta u_j + k_j^2 u = 0 & \text{in } \mathcal{O}_j \\ \partial_n u_2 - ik_2 u_2 = h & \text{on } \partial\mathcal{D} \\ u_2 = u_{\text{obs}} & \text{on } \Gamma_m \\ [u] = [\partial_n u] = 0 & \text{on } \partial\mathcal{O}_1, \end{cases}$$

where $h \in H^{-1/2}(\partial\mathcal{D})$ and $u_{\text{obs}} \in H^{1/2}(\Gamma_m)$ are given and $V = \{u \in H^1(\mathcal{D}) \text{ such that } [u] = 0 \text{ on } \partial\mathcal{O}_1\}$. Here and in all the following, for each quantity o_j defined on a subdomain \mathcal{O}_j , we denote by $[o] = o_1 - o_2$ the jump of o on $\partial\mathcal{O}_1$. In order to simplify the notations, in the following, we also denote by χ_j the characteristic function of \mathcal{O}_j and omitting the subscript implies that we consider the sum $o = \chi_1 o_1 + \chi_2 o_2$. As an important example, k denotes the sum $\chi_1 k_1 + \chi_2 k_2$ and we can write

$$\Delta u + k^2 u = 0 \quad \text{in } \mathcal{D}.$$

Remark 1.1

We underline that, using the Robin boundary condition on $\partial\mathcal{D}$, both Dirichlet u_{obs} and Neumann $\partial_n u_{\text{obs}}$ conditions are known on Γ_m .

2 Main results

In this section, we define the Kohn-Vogelius functional used in this work and state the main theoretical results of this work. First, we calculate its derivative with respect to its two unknowns, that are \mathcal{O}_1 and k_1 . Then, we give a method that takes into account noise on the input data, i.e., the robust method. The general forward problem we aim to solve can be stated as finding functions $u_j \in H^1(\mathcal{O}_j)$ such that

$$\begin{cases} \Delta u + k^2 u = 0 & \text{in } \mathcal{D} \\ \partial_n u - ik_2 u = h & \text{on } \Gamma_c \\ u = u_{\text{obs}} & \text{on } \Gamma_m \\ [u] = 0 & \text{on } \partial\mathcal{O}_1 \\ [\partial_n u] = g & \text{on } \partial\mathcal{O}_1, \end{cases} \quad (\mathcal{T}(\mathcal{O}_1))$$

where $g \in H^{-1/2}(\partial\mathcal{O}_1)$, $h \in H^{-1/2}(\Gamma_c)$ and $u_{\text{obs}} \in H^{1/2}(\Gamma_m)$. The potential errors and uncertainties will occur on the functions h and u_{obs} .

Remark 2.1

A very peculiar case is when Γ_m is empty and $g = 0$. This means that we do not consider any sensors and a transmission condition $[\partial_n u] = 0$, in other words it corresponds to the physical forward case.

The homogeneous forward problem (with $u_{\text{obs}} = 0$) $\mathcal{T}(\mathcal{O}_1)$ writes under variational form as finding $u \in V$ such that

$$\int_{\mathcal{D}} (\nabla u \cdot \nabla \bar{v} - k^2 u \bar{v}) - ik_2 \int_{\partial\mathcal{D}} u \bar{v} = \int_{\partial\mathcal{D}} h \bar{v} + \int_{\partial\mathcal{O}_1} g \bar{v} \quad \text{for all } v \in V,$$

where the notation \bar{v} denotes the complex conjugate of v . Note that since our functions are complex-valued, the scalar product we consider is hermitian.

Proposition 2.2

Under the assumptions above, the transmission problem $(\mathcal{T}(\mathcal{O}_1))$ is well-posed.

Concerning the above inverse problem, we now reformulate it as an optimization problem. We introduce the Kohn-Vogelius (also used in other example as in [11]) functional as follows

$$\mathcal{K}(\mathcal{O}_1, k_1) = \frac{1}{2} \int_{\mathcal{D}} |\nabla(u_D - u_R)|^2, \quad (2.1)$$

where $u_D = u_D(\mathcal{O}_1, k_1) \in V$ and $u_R = u_R(\mathcal{O}_1, k_1) \in V$ are the unique solutions to the problems

$$\begin{cases} \Delta u_D + k^2 u_D = 0 & \text{in } \mathcal{D} \\ \partial_n u_D - ik_2 u_D = h & \text{on } \Gamma_c \\ u_D = u_{\text{obs}} & \text{on } \Gamma_m \\ [u_D] = [\partial_n u_D] = 0 & \text{on } \partial\mathcal{O}_1, \end{cases} \quad \begin{cases} \Delta u_R + k^2 u_R = 0 & \text{in } \mathcal{D} \\ \partial_n u_R - ik_2 u_R = h & \text{on } \partial\mathcal{D} \\ [u_R] = [\partial_n u_R] = 0 & \text{on } \partial\mathcal{O}_1. \end{cases} \quad (2.2)$$

The cost functional \mathcal{K} has two parameters \mathcal{O}_1 and k_1 that correspond to our two unknowns. By the proposition above, the equations defining u_D and u_R are well posed. We see that the solutions to the inverse problem minimize the functional as they are zeros of \mathcal{K} . However, we do not know if all minimizers are solutions

to the inverse problem. This question is related to the identifiability of the problem: *is knowing h and g enough to determine \mathcal{O}_1 and k_1 ?* If we consider another problem, such as the perfectly electric conductor (PEC), i.e. $u = 0$ on $\partial\mathcal{O}_1$, the identifiability can be proved adapting the property 4.4 of [17]. In the context of thin-layer and reconstructing the impedance, Bourgeois *et al.* showed in [5] that identifiability holds in the case where all observation and scattering directions are known.

In the following, we aim to use an iterative Nesterov scheme (see section 4 for more details) to minimize the previous functional. To do so, we need to compute a gradient at each iteration with respect to both the shape \mathcal{O}_1 and the wavenumber k_1 . To calculate the shape gradient, we use the classical notion of shape derivative, that we briefly recall here (see [24]).

Definition 2.3 (Shape derivative)

Let $J : \mathcal{D}_{adm} \rightarrow \mathbb{R}$ be a functional defined on a class of admissible shapes \mathcal{D}_{adm} . Let \mathcal{W} be a functional subspace of $W^{1,\infty}(\mathbb{R}^d)$ and denote the identity $\mathbb{R}^d \rightarrow \mathbb{R}^d$ by I . The shape derivative of J at \mathcal{O} is the Fréchet derivative of

$$\begin{cases} \mathcal{W} \rightarrow \mathbb{R} \\ \theta \mapsto J((I + \theta)(\mathcal{O})) \end{cases}$$

if it exists. It will be denoted in the following by $D_{\mathcal{O}_1}\mathcal{J}(\mathcal{O})(\theta)$.

In this article, the functional subspace W used in the proof is $W_0^{1,\infty}(\mathcal{D})$. It is the subspace of $W^{1,\infty}(\mathbb{R}^d)$, made of functions with traces that vanish on $\partial\mathcal{D}$.

2.1 Deterministic case

We begin by giving the expression of the derivatives of \mathcal{K} with respect to both the wavenumber k_1 and the shape \mathcal{O}_1 in the deterministic case.

Proposition 2.4 (Derivative with respect to \mathcal{O}_1)

Let $k_1 \in \mathfrak{K}_{adm}$. For every $\mathcal{O}_1 \in \mathcal{U}_{adm}$, and $\theta \in W_0^{1,\infty}(\mathcal{D})$, the shape derivative of the Kohn-Vogelius functional can be expressed as follows

$$D_{\mathcal{O}_1}\mathcal{K}(\mathcal{O}_1, k_1)(\theta) = \Re \left(\int_{\partial\mathcal{O}_1} (k_1^2 - k_2^2)(u_D\rho_D - u_R\rho_R)(\theta \cdot n) \right),$$

where $\rho_D \in V$ and $\rho_R \in V$ are solutions to the adjoint equations

$$\begin{cases} \Delta\rho_D + k^2\rho_D = -\bar{k}^2(\overline{u_D - u_R}) & \text{in } \mathcal{D} \\ \partial_n\rho_D - ik\rho_D = \partial_n(u_D - u_R) & \text{on } \Gamma_c \\ \rho_D = 0 & \text{on } \Gamma_m \\ [\rho_D] = [\partial_n\rho_D] = 0 & \text{on } \partial\mathcal{O}_1, \end{cases} \quad \begin{cases} \Delta\rho_R + k^2\rho_R = -\bar{k}^2(\overline{u_D - u_R}) & \text{in } \mathcal{D} \\ \partial_n\rho_R - ik\rho_R = \partial_n(u_D - u_R) & \text{on } \partial\mathcal{D} \\ [\rho_R] = [\partial_n\rho_R] = 0 & \text{on } \partial\mathcal{O}_1. \end{cases} \quad (2.3)$$

Proposition 2.5 (Derivative with respect to k)

Let $\mathcal{O}_1 \in \mathcal{U}_{adm}$. For every $k_1 \in \mathfrak{K}_{adm}$, the derivative of the Kohn-Vogelius functional (2.1) with respect to k_1 exists and

$$\frac{\partial\mathcal{K}(\mathcal{O}_1, k_1)}{\partial k_1} = 2 \int_{\mathcal{O}_1} (\rho_D u_D - \rho_R u_R) k_1,$$

where $u_D \in V$ and $u_R \in V$ are defined in the equations (2.2) and $\rho_D \in V$ and $\rho_R \in V$ are solutions to the previous equations (2.3).

2.2 Case with uncertainties

The method detailed above is considered under ideal conditions, i.e., a deterministic case where the quantities u_{obs} and h are known with precision. In practice, however, this is not the case. Two factors compromise

the effectiveness of our approach. First, there is a noise on u_{obs} which arise from measurements. Second, h depends on the incident wave vector that may deviate from our exact expectations.

In order to take into account those uncertainties, we consider a stochastic framework where we assume that the errors follow a statistical law. Precisely, we let $(\Omega, \mathcal{T}, \mathbb{P})$ be a probability space, $h \in L^2_{\mathbb{P}}(\Omega, H^{-1/2}(\partial\mathcal{D}))$ and $u_{\text{obs}} \in L^2_{\mathbb{P}}(\Omega, H^{1/2}(\Gamma_m))$. For a given $\omega \in \Omega$, the inverse problem in the first strategy can be rewritten as finding $\mathcal{O}_1 \in \mathcal{U}_{\text{adm}}$, $k_1 \in \mathcal{K}_{\text{adm}}$ and $u(\omega) \in V$ such that

$$\begin{cases} \Delta u(\omega) + k^2 u(\omega) = 0 & \text{in } \mathcal{D} \\ \partial_n u(\omega) - iku(\omega) = h(\omega) & \text{on } \partial\mathcal{D} \\ u(\omega) = u_{\text{obs}}(\omega) & \text{on } \Gamma_m \\ [u(\omega)] = [\partial_n u(\omega)] = 0 & \text{on } \partial\mathcal{O}_1. \end{cases}$$

In practice, the main difficulty lies in the fact that we know only the realizations of the random variables u_{obs} and h . There are many ways to solve the problem with uncertainties. We could use a Monte-Carlo method or a stochastic gradient descent, but it would lead to very long computation time. To overcome this problem, we choose to minimize a combination of the expected value and the variance of the considered functional \mathcal{K} , that is to say we are considering

$$\tilde{\mathcal{K}}(\mathcal{O}_1, k_1, \omega) = (1 - \alpha)\mathbb{E}(\mathcal{K}(\mathcal{O}_1, k_1, \omega)) + \alpha\mathbb{V}(\mathcal{K}(\mathcal{O}_1, k_1, \omega)),$$

for $\alpha \in [0, 1]$. Hence, the problem is reduced to a purely deterministic problem which can be treated as before. For this purpose, we rely on a truncated Karhunen-Loëve expansion (see [21, 16] for more details). Let $M > 0$ be an integer, Y be a centered and normalized random variable with all the moments of order lower than 4 finite. We consider M independent and identically distributed random variables $Y_i \sim Y$, $(g_m)_{1 \leq m \leq M} \in H^{1/2}(\Gamma_m)$ and $(h_m)_{1 \leq m \leq M} \in H^{-1/2}(\Gamma_m)$ such that

$$u_{\text{obs}}(x, \omega) = g_0(x) + \sum_{m=1}^M g_m(x)Y_m(\omega) \quad \text{and} \quad h(x, \omega) = h_0(x) + \sum_{m=1}^M h_m(x)Y_m(\omega). \quad (2.4)$$

By linearity of the Helmholtz equation, we get

$$u_R(\omega) = u_{R_0} + \sum_{m=1}^M u_{R_m} Y_m(\omega) \quad \text{and} \quad u_D(\omega) = u_{D_0} + \sum_{m=1}^M u_{D_m} Y_m(\omega),$$

where $u_{D_m} \in V$ and $u_{R_m} \in V$ solve for all $0 \leq m \leq M$,

$$\begin{cases} \Delta u_{D_m} + k^2 u_{D_m} = 0 & \text{in } \mathcal{D} \\ \partial_n u_{D_m} - iku_{D_m} = h_m & \text{on } \Gamma_c \\ u_{D_m} = g_m & \text{on } \Gamma_m \\ [u_{D_m}] = [\partial_n u_{D_m}] = 0 & \text{on } \partial\mathcal{O}_1, \end{cases} \quad \begin{cases} \Delta u_{R_m} + k^2 u_{R_m} = 0 & \text{in } \mathcal{D} \\ \partial_n u_{R_m} - iku_{R_m} = h_m & \text{on } \partial\mathcal{D} \\ [u_{R_m}] = [\partial_n u_{R_m}] = 0 & \text{on } \partial\mathcal{O}_1. \end{cases}$$

We can compute $\mathbb{E}(\mathcal{K}(\mathcal{O}_1, k_1, \omega))$ and $\mathbb{V}(\mathcal{K}(\mathcal{O}_1, k_1, \omega))$ in any cases, but we will consider the case $Y \sim \mathcal{N}(0, 1)$ to simplify the expressions of the variance in the following.

Proposition 2.6 (Expression of the expected value of the functional)

In the framework described above, we have

$$\mathcal{E}_{\mathcal{K}}(\mathcal{O}_1, k_1) = \mathbb{E}(\mathcal{K}(\mathcal{O}_1, k_1, \omega)) = \frac{1}{2} \int_{\mathcal{D}} \sum_{m=0}^M |\nabla(u_{D_m} - u_{R_m})|^2.$$

For $\theta \in W_0^{1,\infty}(\mathbb{R}^d)$, $\mathcal{O}_1 \in \mathcal{U}_{\text{adm}}$ and $k_1 \in \mathcal{K}_{\text{adm}}$, the derivatives given by the adjoint exist and are given by

$$D_{\mathcal{O}_1} \mathcal{E}_{\mathcal{K}}(\mathcal{O}_1, k_1)(\theta) = \sum_{m=0}^M \Re \left(\int_{\partial\mathcal{O}_1} (k_1^2 - k_2^2)(u_{D_m} \rho_{D_m} - u_{R_m} \rho_{R_m})(\theta \cdot n) \right),$$

$$\frac{\partial \mathcal{E}_K(\mathcal{O}_1, k_1)}{\partial k_1} = 2 \sum_{m=0}^M \int_{\mathcal{O}_1} (\rho_{D_m} u_{D_m} - \rho_{R_m} u_{R_m}) k_1, \quad (2.5)$$

where $\rho_{D_m} \in V$ and $\rho_{R_m} \in V$ solve, for all $1 \leq m \leq M$,

$$\begin{cases} \Delta \rho_{D_m} + k^2 \rho_{D_m} = -\bar{k}^2 (u_{D_m} - u_{R_m}) & \text{in } \mathcal{D} \\ \partial_n \rho_{D_m} - ik \rho_{D_m} = \partial_n (u_{D_m} - u_{R_m}) & \text{on } \Gamma_c \\ \rho_{D_m} = 0 & \text{on } \Gamma_m \\ [\rho_{D_m}] = [\partial_n \rho_{D_m}] = 0 & \text{on } \partial \mathcal{O}_1, \end{cases} \quad \begin{cases} \Delta \rho_{R_m} + k^2 \rho_{R_m} = -\bar{k}^2 (u_{D_m} - u_{R_m}) & \text{in } \mathcal{D} \\ \partial_n \rho_{R_m} - ik \rho_{R_m} = \partial_n (u_{D_m} - u_{R_m}) & \text{on } \partial \mathcal{D} \\ [\rho_{R_m}] = [\partial_n \rho_{R_m}] = 0 & \text{on } \partial \mathcal{O}_1. \end{cases}$$

Proposition 2.7 (Expression of the variance of the functional)

We introduce the notation $d_i = u_{R_i} - u_{D_i}$ and $p_{j,i} = u_{D_i} \rho_{D_j} - u_{R_i} \rho_{R_j}$. Let $\mathcal{O}_1 \in \mathcal{U}_{\text{adm}}$, $k_1 \in \mathfrak{K}_{\text{adm}}$. In the framework described above, if $Y \sim \mathcal{N}(0, 1)$, we have

$$\begin{aligned} \mathcal{V}_K(\mathcal{O}_1, k_1) = \mathbb{V}(\mathcal{K}(\mathcal{O}_1, k_1, \omega)) &= \frac{1}{4} \left(\int_{\mathcal{D}} |\nabla d_0|^2 \right)^2 + \frac{1}{2} \left(\int_{\mathcal{D}} |\nabla d_0|^2 \right) \left(\sum_{m=1}^M \int_{\mathcal{D}} |\nabla d_m|^2 \right) \\ &+ \sum_{m=1}^M \left(\int_{\mathcal{D}} \Re(\nabla d_0 \cdot \nabla \overline{d_m}) \right)^2 + \Re \left(\sum_{1 \leq m < l \leq M} \left(\int_{\mathcal{D}} \nabla d_m \nabla \overline{d_l} \right)^2 \right) + \frac{1}{2} \sum_{m=1}^M \left(\int_{\mathcal{D}} |\nabla d_m|^2 \right)^2. \end{aligned} \quad (2.6)$$

For $\theta \in W_0^{1,\infty}(\mathcal{D})$, the derivatives given by the adjoint method are now

$$D_{\mathcal{O}_1} \mathcal{V}_K((\mathcal{O}_1, k_1))(\theta) = \Re \left(\int_{\partial \mathcal{O}_1} (k_1^2 - k_2^2) \mathcal{G}(\theta \cdot n) \right) \quad \text{and} \quad \frac{\partial \mathcal{V}_K(\mathcal{O}_1, k_1)}{\partial k_1} = 2 \int_{\mathcal{O}_1} \mathcal{G} k_1$$

where

$$\begin{aligned} \mathcal{G} &= \frac{1}{2} \left(\int_{\mathcal{D}} |\nabla d_0|^2 \right) \sum_{m=1}^M p_{m,m} + 2 \sum_{m=1}^M \left(\int_{\mathcal{D}} \Re(\nabla d_0 \cdot \nabla \overline{d_m}) \right) p_{0,m} \\ &+ 4 \sum_{1 \leq m < l \leq M} \Re \left(\int_{\mathcal{D}} \nabla d_m \nabla \overline{d_l} \right) p_{m,l} + \sum_{m=1}^M \left(\int_{\mathcal{D}} |\nabla d_m|^2 \right) p_{m,m}. \end{aligned} \quad (2.7)$$

3 Numerical experiments

To illustrate the effectiveness of our approach, we present numerical experiments in 2D.

3.1 Algorithm

To ensure visibility of the unknown target, we consider different incidents directions θ_j for $1 \leq j \leq J$. For each direction, we take

$$h^j = i(k - k_{\text{inc}}^j(\theta_j) \cdot n) u_{i_0} \exp(-ik_{\text{inc}}^j(\theta_j) \cdot r),$$

where k_{inc}^j corresponds to the incident wave vector given by $k_{\text{inc}}^j = -k(\cos(\theta_j), \sin(\theta_j))$. It is important to note that we have in total J functionals rather than a single one. We chose to minimize each functional successively over a given number of iterations. Our method consists of a sequential process: we begin by minimizing with respect to the first direction of the plane wave, then the second, and so on, until all directions have been considered. This cycle is then repeated, starting again with the first direction. The descent method used in the following is the Nesterov's accelerated gradient scheme [27]:

$$\begin{cases} x_{n+1} = y_n - \tau_{\mathcal{O}_1, k_1} \nabla f(y_n) \\ y_{n+1} = x_{n+1} + \frac{\eta_t - 1}{\eta_{t+1}} (x_{n+1} - x_n), \quad y_0 = x_0 \\ \eta_{t+1} = \frac{1 + \sqrt{1 + 4\eta_t^2}}{2}, \quad \eta_0 = 1, \end{cases}$$

with restarting [28]: if $\mathcal{K}(x_{n+1}) > \mathcal{K}(x_n)$, we take $\eta_0 = 1$, $x_0 = x_n$, $y_0 = x_n$. The variables in the algorithm (e.g. x_n and y_n) are vectors of size 2 of the form $[\mathcal{O}_1, k_1]$ and the step time τ is $\tau_{\mathcal{O}_1, k_1} = [\tau_{\mathcal{O}_1}, \tau_{k_1}]$. Hence, both shape and parameters are updated at each iteration at the same time, with their own gradient and step τ .

The choice of the two descents step is a key point of our algorithm. If the step size are too large, the process becomes unstable, potentially leading to divergence or even failure to converge at all. On the other hand, if the step sizes are too small, the reconstruction becomes excessively slow.

In addition, we consider a truncated Fourier series parametrization for the boundary of the object \mathcal{O}_1 :

$$\partial\mathcal{O}_1 = \begin{bmatrix} x_c \\ y_c \end{bmatrix} + \left(r + \sum_{n=1}^N a_n \cos(n\theta) + b_n \sin(n\theta) \right) \begin{bmatrix} \cos(\theta) \\ \sin(\theta) \end{bmatrix}.$$

To avoid the instability of the inverse problem, the Fourier coefficients are introduced incrementally. The first five iterations are used to adjust the center. The radius is introduced after this fifth iteration, and each subsequent Fourier coefficient is added at multiples of 30 iterations. Hence, the more iterations we do, the bigger is the number of Fourier coefficients we accumulate by the end of our algorithm. Note that we could also choose to add them following a criterion, such as adding some coefficients if the functional is not changing over a certain number of iterations. Nonetheless, the goal here is to validate the method. The general idea of the proposed scheme is summed up in the pseudo-code 1.

Algorithm 1 Descent algorithm

```

Require:  $N_{\text{iter}}$ ,  $N_{\text{seq}}$ ,  $\theta_{\text{inc}}$ 
for  $0 \leq n < N_{\text{iter}}$  do
  for  $\theta_j \in \theta_{\text{inc}}$  do
    Nesterov scheme with  $N_{\text{seq}}$  iterations and the functional  $\mathcal{K}^j$ 
  end for
end for
end for

```

3.2 Implementation

We conduct numerical experiments to assess the effectiveness of the different methods developed earlier in section 2. We use the PDE solver FreeFEM++ (see [23]) and the package pyfreefem (see [22]) to interface with Python. The FreeFEM++ version we use is parallelized using the MPI library. The resolution of the inverse problem requires a high-performance computing (HPC) cluster, specifically Pyrene developed at the Université de Pau. The forward problem is first modeled using P2 finite elements on a highly refined mesh. The solution is then computed on a new mesh with P1 finite elements to avoid the inverse crime problem.

We use the parallelization for the robust case only. It is implemented as a process distribution, where each process corresponds to a term in the Karhunen–Loëve expansion (2.4). Thanks to this method, we were able to increase the order of the expansion while maintaining approximately the same computation time. With 5 terms in the expansion, each iteration requires approximately 60s.

3.3 Results

In all the experiences below, we consider a general domain \mathcal{D} , which is modeled as a disk of radius 1. We consider four incident waves coming from directions $\theta_i = 0, \frac{\pi}{2}, \pi$ and $\frac{3\pi}{2}$, with each having the same amplitude of 1 and the same frequency $f = 1$ MHz. The space of measures Γ_m is constituted of six uniformly distributed intervals on the boundary of \mathcal{D} . In the following, our main objective is to reconstruct a shape that does not enter into our Fourier parametrizations. We will name it the "kite" and it can be parameterized by

$$\begin{bmatrix} x \\ y \end{bmatrix} = \begin{bmatrix} 0.3 \cos(t) + 0.2 \cos(2t) \\ 0.4 \sin(t) \end{bmatrix}.$$

For the object we consider a wavenumber, k_1 , associated to a permittivity $\varepsilon = 50 + 29j$. The outside permittivity is taken $\varepsilon = 10 + 4j$. The initial guess for the shape is a disk with a radius of 0.6. The descent is performed with a total of 400 iterations, with $N_{\text{iter}} = 4$ descent directions, $N_{\text{seq}} = 25$ sequential step per direction, and a step size of 0.02.

3.3.1 Deterministic reconstruction

Deterministic reconstruction of the shape at fixed wavenumber. First, we aim to reconstruct the shape assuming that we know the wavenumber. Hence, we take k_1 as the initial wavenumber and attempt to reconstruct the kite shape. The results, depicted in Figure 2, show the final retrieved shape (orange, dashed) closely approximately the true kite geometry (plain). In Figure 2, we also represent the evolution of the functional. The initial shape is represented in dotted. All the figures represented will have the same convention.

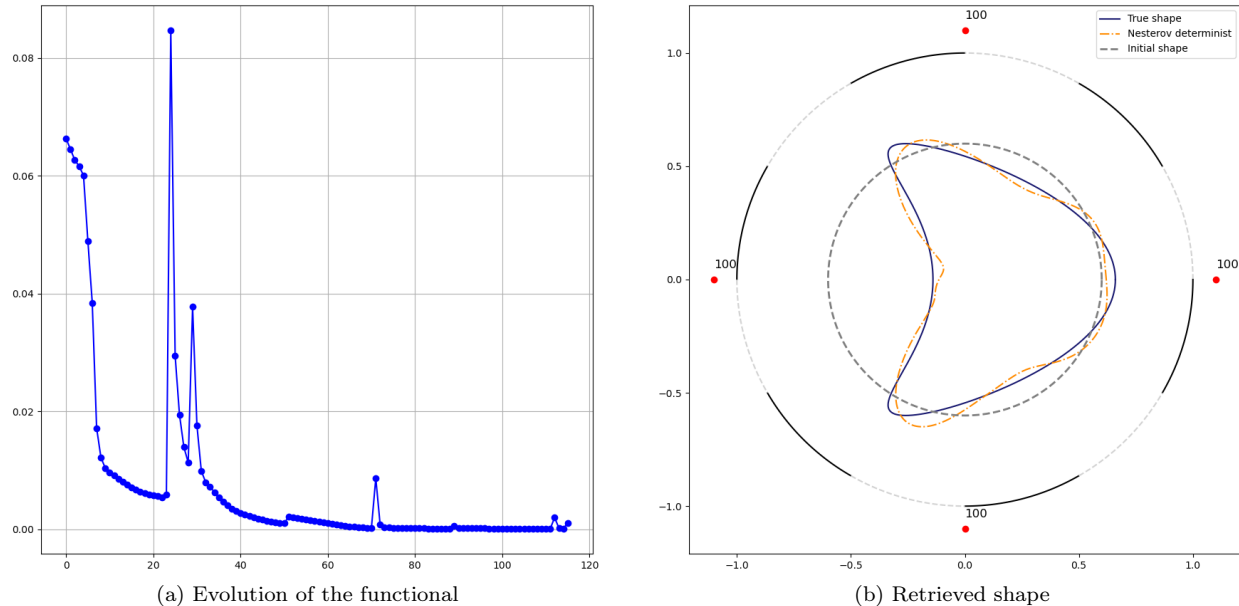


Figure 2: Reconstruction of the shape at fixed wavenumber

The objective functional does not decrease monotonically. Indeed, the functional we minimize along the descent depends on the incident direction. Hence, we can observe some jumps in the functional decrease. They correspond to the changes of initial direction. Moreover, the difference between the total number of iterations (400) and the number of points plotted is due to the removal of certain iterations at restart points within the algorithm. Nevertheless, we can see that the functional decreases globally and converges to 0 with the number of iterations. All the other experiments have a similar behaviour for the functional.

Determinist reconstruction of the wavenumber at fixed shape. We also attempted to reconstruct the wavenumber k_1 using the unknown as the initial shape. Initially, we set the shape update step $\tau_{\mathcal{O}_1}$ to 0, so that the algorithm is a Nesterov descent on the parameter k only. In this experience only, the objective shape is the initial shape: the disk of radius 0.6. Also, we have chosen $N_{\text{iter}} = 1$. However, this intuitive approach failed. We observed that the functional J is extremely sensitive to the unknown shape (we refer to [18, Section 4.3] where this observation was done in another context). Indeed retrieving the permittivity is a very ill-posed inverse problem in general. In particular, in our setting, i.e., the size of the object of around $\lambda/300$, we are in the Rayleigh diffraction zone where the scattering waves variations are dominated by the area of the target. Therefore, this sensitivity suggests that even very small shape variations of the shape (for instance, those introduced by copying the shape to a new mesh) result in large

variations in J . Our solution was to consider a very small step for the shape update (0.0001) compared to the wavenumber update (0.4). This strategy keeps the shape very close to the true one. We tested this with two initial wavenumbers: $0.9k_1$ and $1.2k_1$. All the other parameters remain the same. In Figure 3, we plot the evolution of the real and imaginary parts of the wavenumber during the reconstruction.

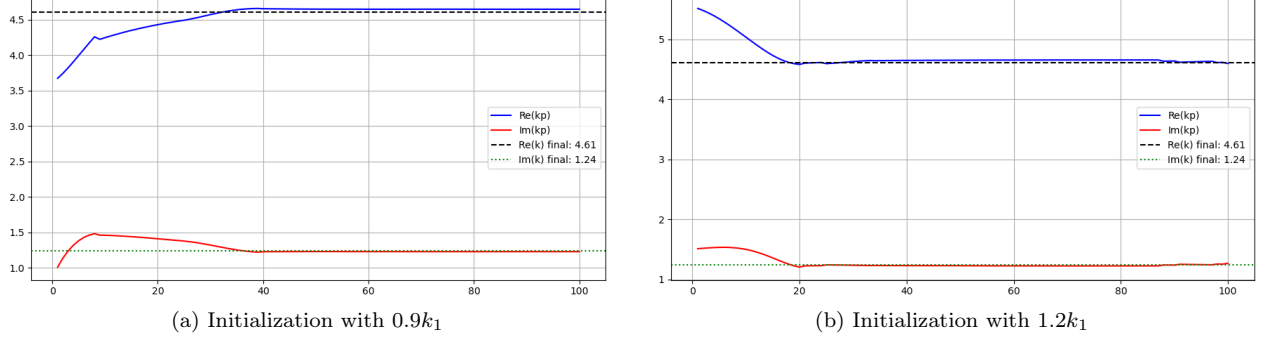


Figure 3: Reconstruction of the wavenumber at fixed shape

We can notice that the results are very accurate in both cases, even if no regularization is performed. Furthermore, this highlight the importance of the proposed dual strategy, i.e., incorporating the shape reconstruction, for the inverse scattering problem. It shall also be noted that obstacle detection and reconstruction at low frequency is of interest for the electromagnetic community [29].

3.3.2 Reconstruction with uncertainties:

Simultaneous reconstruction with uncertainties and the expected value: We now attempt the simultaneous reconstruction of both the shape and the parameter with noisy data. To do so, h_0 is assumed to be the deterministic data, with g_0 being the associated observation u_{obs} . Then, we consider g_m and h_m of the following forms:

$$g_m = \beta_g \sin(m\phi) \quad \text{and} \quad h_m = \beta_h \sin(k\phi) i(k - k_{\text{inc}}^j(\theta_j) \cdot n) \exp(-ik_{\text{inc}}^j(\theta_j) \cdot r),$$

where (ϕ, r) are the usual polar coordinates.

We first consider the minimization of the expected value only. We investigate one case with 5% of noise on g and 1% on h , and conversely 1% of noise on g and 5% on h , see 5. By "percentage of noise," we refer to the noise level relative to the squared of the L^2 -norm on the boundary. Thus, β_g and β_h were chosen to match these expected noise percentages. As an example, 5% of noise on g and 1% on h correspond to

$$0.05^2 = \beta_g \mathbb{E} \left(\frac{\|g_1 + g_2 + g_3 + g_4\|_{L^2(\Gamma_m)}^2}{\|g_0\|_{L^2(\partial D)}^2} \right)$$

and

$$0.01^2 = \beta_h \mathbb{E} \left(\frac{\|h_1 + h_2 + h_3 + h_4\|_{L^2(\partial D)}^2}{\|h\|_{L^2(\partial D)}^2} \right).$$

In Figure 4, we represent the final shape and the evolution of the wavenumber for both experiments. With these levels of noise, we see that the method is able to retrieve both shape and wavenumber and remain robust under uncertainties.

Simultaneous reconstruction with uncertainties by minimization of the expected value and variance: Lastly, we put 3% of errors on both h and g and consider 3 different combinations of expected value and variance. Hence, the functional considered is

$$\mathcal{J} = (1 - \alpha)\mathcal{E}_K(\mathcal{O}_1, k_1) + \alpha\mathcal{V}_K(\mathcal{O}_1, k_1).$$

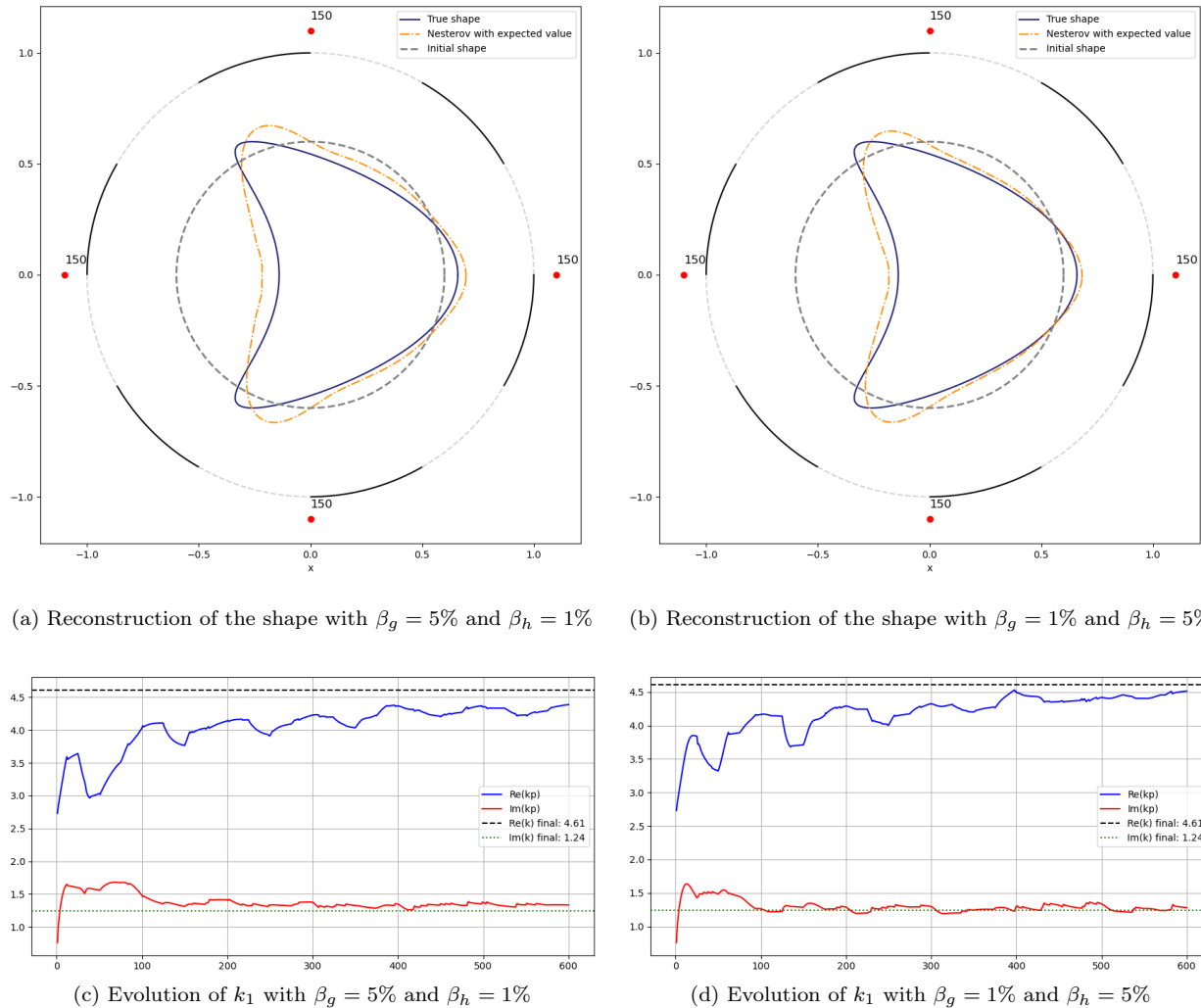


Figure 4: Simultaneous reconstruction with noisy data and minimization of the expected value.

In Figure 5, we represent the final shape for the three values of α . In Figure 6, we represent the evolution of the real parts of the wavenumber for the three experiments.

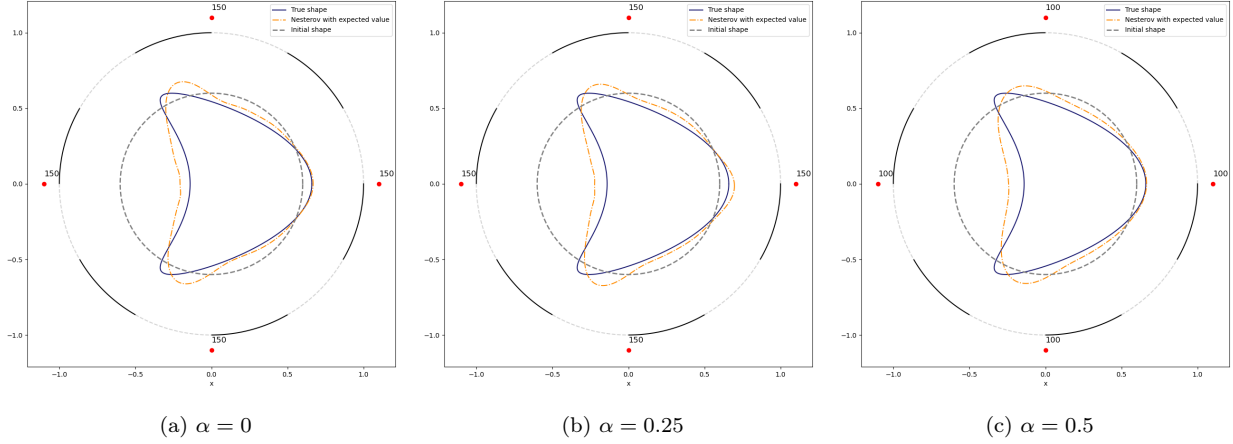


Figure 5: Simultaneous reconstruction with noisy data and a linear combination of the wavenumber and variance

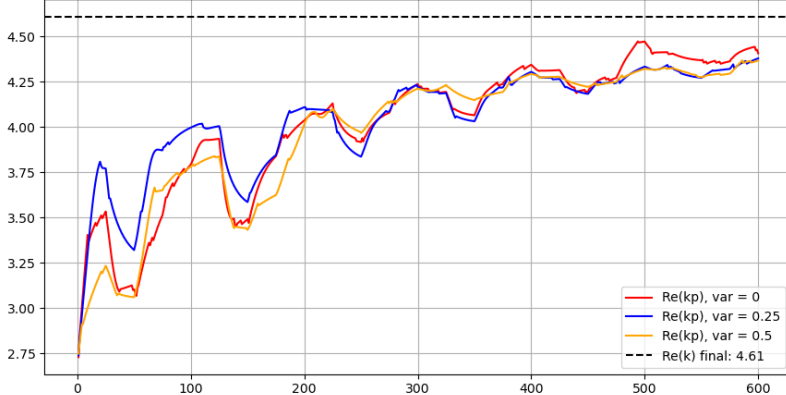


Figure 6: Simultaneous reconstruction of the wavenumber with noisy data and a linear combination of the wavenumber and variance

We observe that increasing the value of α smooths the reconstructed shape, leading to a slightly worse reconstruction. On the other hand, the wavenumber becomes more stable with increasing variance. This tests show that the variance act as a regularizer for the robust approach and thus the choice of a good α is critical.

4 Proofs

In this section, we provide the proofs of the propositions stated above.

4.1 Proof of the well-posedness of the problem $\mathcal{T}(\mathcal{O}_1)$

We present the proof in the particular case where $g = 0$ and Γ_m is empty, which corresponds to the forward physical equation with Robin boundary conditions only. The results, however, remain valid in full generality, up to a modification of the linear form l in the proof. Hence, all the problems considered in this paper are

well-defined including the adjoint problems. We remind first two results of elliptic PDEs used in the following proof.

Theorem 4.1 (Banach-Nečas-Babuska Theorem (BNB), [20, Theorem 25.9])

Let V be a Banach space, W be a reflexive Banach space and $a \in \mathcal{L}(V \times W, \mathbb{C})$. The following items are equivalent:

1. For any $l \in W'$, there exists a unique $u \in V$ such that

$$a(u, w) = l(w), \text{ for all } w \in W.$$

2. There exists $\beta > 0$ such that $\inf_{v \in V} \sup_{w \in W} \frac{a(v, w)}{\|w\|_W} = \beta$ and $(\forall v \in V, a(v, w) = 0 \Rightarrow (w = 0))$.

3. There exists $\beta_1, \beta_2 > 0$ such that $\inf_{v \in V} \sup_{w \in W} \frac{a(v, w)}{\|v\|_V \|w\|_W} = \beta_1$ and $\inf_{w \in W} \sup_{v \in V} \frac{a(v, w)}{\|v\|_V \|w\|_W} = \beta_2$.

We also have a lemma that provides a sufficient condition for applying the BNB:

Lemma 4.2 (Gårding's lemma, [20, Lemma 35.3])

Let $V \hookrightarrow L$ be two Banach spaces with compact embedding. Let $a : V \times V \rightarrow \mathbb{C}$ be a bounded sesquilinear form. Assume that there exist two real numbers $\beta, \gamma > 0$ such that the following holds:

1. $|a(v, v)| + \beta \|v\|_L^2 \geq \gamma \|v\|_V^2, \forall v \in V$
2. $[a(v, w) = 0, \forall w \in V] \Rightarrow (v = 0)$.

Then the second condition of the BNB Theorem is satisfied.

Proof of the well-posedness of the problem $\mathcal{T}(\mathcal{O}_1)$. To prove this we make use of the Lemma 4.2 and thus prove its two points.

1. Let us denote $A(u, v) = \int_{\mathcal{D}} \nabla u \nabla \bar{v} - k^2 u \bar{v} - ik_2 \int_{\partial\mathcal{D}} u \bar{v}$ and consider $\Re(A(u, -ik_2 u))$.

$$\begin{aligned} & \Re(A(u, -ik_2 u)) \\ &= \Re \left(i \left[\overline{k_2} \|\nabla u\|_{L^2(\mathcal{O}_1)}^2 + \overline{k_2} \|\nabla u\|_{L^2(\mathcal{O}_2)}^2 - k_1^2 \overline{k_2} \|u\|_{L^2(\mathcal{O}_1)}^2 - k_2^2 \overline{k_2} \|u\|_{L^2(\mathcal{O}_2)}^2 \right] + |k_2|^2 \|u\|_{L^2(\partial\mathcal{D})}^2 \right) \\ &= \Im(k_1^2 \overline{k_2}) \|u\|_{L^2(\mathcal{O}_1)}^2 + \Im(k_2) \left[\|\nabla u\|_{L^2(\mathcal{D})}^2 + \|k_2 u\|_{L^2(\mathcal{O}_2)}^2 \right] + |k_2|^2 \|u\|_{L^2(\partial\mathcal{D})}^2. \end{aligned}$$

Hence, with the definition of $\mathfrak{K}_{\text{adm}}$,

$$|k_2| |A(u, u)| + |\Im(k_1^2 \overline{k_2})| \|u\|_{L^2(\mathcal{O}_1)}^2 \geq \Im(k_2) \left[\|\nabla u\|_{L^2(\mathcal{D})}^2 + \|k_2 u\|_{L^2(\mathcal{O}_2)}^2 \right] + |k_2|^2 \|u\|_{L^2(\partial\mathcal{D})}^2$$

and we get the first point of the Gårding's lemma.

2. For the second point, assume that $A(u, v) = 0$ for every $v \in V$. Hence,

$$\Im(A(u, u)) = -\Re(k_2) (\|u\|_{L^2(\partial\mathcal{D})} + 2\Im(k_2) \|u\|_{L^2(\mathcal{O}_2)}) - 2\Re(k_1) \Im(k_1) \|u\|_{L^2(\mathcal{O}_1)} = 0$$

and, since $\Im(k_1) > 0$ and the real parts $\Re(k_1)$ and $\Re(k_2)$ have the same sign, we obtain $\|u\|_{L^2(\partial\mathcal{D})} = 0$. By the Robin condition $\partial_n u = 0$ on $\partial\mathcal{D}$ and u is solution of the Cauchy problem for the Helmholtz equation in \mathcal{O}_2 . The jump condition on $\partial\mathcal{O}_1$ shows that u is also solution of the Cauchy problem for the Helmholtz equation in \mathcal{O}_1 and that $u \equiv 0$ in \mathcal{D} . \square

4.2 Reminder on shape optimization

First, we remind two important lemmas that are necessary for the following proof.

Lemma 4.3

Let $J : \mathcal{D}_{adm} \rightarrow \mathbb{R}$ be a functional defined on a class of admissible shapes \mathcal{D}_{adm} . Let $\theta \in W_0^{1,\infty}(\mathcal{D})$ and $f \in L^1(\mathbb{R}^d)$. If $J(\mathcal{O}_\theta) = \int_{\mathcal{O}_\theta} f(\theta)$, then

$$J'(\mathcal{O})(\theta) = \int_{\mathcal{O}} f'(x) + \int_{\partial\mathcal{O}} f(\theta \cdot n),$$

where $f'(x)$ denotes the Fréchet derivative of the map $\theta \mapsto f(x + \theta(x))$.

Proof. This is the result [24, corollary 5.2.8] from the book of Henrot and Pierre applied with $\Phi(x) = (I + t\theta(x))$. \square

Lemma 4.4 (Lemma 5.3.3 [24])

Let $\psi : W^{1,\infty}(\mathbb{R}^d) \rightarrow W^{1,\infty}(\mathbb{R}^d)$ continuous at 0 with $\psi(0) = I$ and $g : W^{1,\infty}(\mathbb{R}^d) \rightarrow W^{1,p}(\mathbb{R}^d)$, with $1 \leq p < +\infty$. If $\theta \mapsto (g(\theta), \psi(\theta)) \in L^p(\mathbb{R}^d) \times L^\infty(\mathbb{R}^d)$ is differentiable at 0 with $g'(0)$ continuous, then the application

$$G : \theta \in W^{1,\infty}(\mathbb{R}^d) \mapsto g(\theta) \circ \psi(\theta) \in L^p(\mathbb{R}^d)$$

is differentiable at 0 and

$$G'(0)\xi = g'(0)\xi + \nabla g(0) \cdot \psi'(0)\xi.$$

4.3 Proofs concerning the deterministic case

The proof of the proposition 2.4 is divided into two steps. First, we classically differentiate the functional \mathcal{K} using the technical lemmas recalled in the last subsection. We obtain an expression which is not satisfactory from a numerical point of view. Indeed, in order to apply a Nesterov descent scheme, we need to efficiently compute a clear direction of descent. Thus, the second step of the proof consists in introducing adjoints in order to establish the proposition 2.4.

Lemma 4.5

For every \mathcal{O} admissible, and $\theta \in W_0^{1,\infty}(\mathcal{D})$ the shape derivative of the functional (2.1) exists and

$$D_{\mathcal{O}_1}\mathcal{K}(\mathcal{O}_1, k_1)(\theta) = \Re \left(\int_{\mathcal{D}} \nabla(u'_D - u'_R) \cdot \nabla(\bar{u}_D - \bar{u}_R) \right), \quad (4.1)$$

where $u'_R \in H^1(\mathcal{D})$ and $u'_D \in H^1(\mathcal{D})$ are solutions to

$$\begin{cases} \Delta u'_R + k^2 u'_R = 0 & \text{in } \mathcal{D} \\ \partial_n u'_R - iku'_R = 0 & \text{on } \partial\mathcal{D} \\ [u'_R] = 0 & \text{on } \partial\mathcal{O}_1 \\ [\partial_n u'_R] = (k_1^2 - k_2^2)u_R(\theta \cdot n) & \text{on } \partial\mathcal{O}_1, \end{cases} \quad \begin{cases} \Delta u'_D + k^2 u'_D = 0 & \text{in } \mathcal{D} \\ \partial_n u'_D - iku'_D = 0 & \text{on } \Gamma_c \\ u'_D = 0 & \text{on } \Gamma_m \\ [u'_D] = 0 & \text{on } \partial\mathcal{O}_1 \\ [\partial_n u'_D] = (k_1^2 - k_2^2)u_D(\theta \cdot n) & \text{on } \partial\mathcal{O}_1. \end{cases}$$

The proof of this lemma is similar to the one proposed by Afraites and Dambrine in [1, Theorem 3.1] for a different problem. However, our weak formulation differs and we have to proceed differently for the steps 2 and 3 of their proof. The main difference to the proof of Afraites and Dambrine is that $\frac{w(t)-u}{t}$ does not belong to the space V and we cannot demonstrate its weak convergence as they do. Therefore, we directly prove that it converges strongly to a chosen quantity.

Proof of the lemma 4.5. Fix $\mathcal{O} \in \mathcal{U}_{\text{adm}}$ and $\theta \in W_0^{1,\infty}(\mathcal{D})$. We denote by $u_D(\theta)$ and $u_R(\theta)$ the solutions to the problems (2.2) with $\mathcal{O}_1 = (I + \theta)(\mathcal{O})$. We only need to prove that $\theta \mapsto u_R(\theta)$ and $\theta \mapsto u_D(\theta)$ have shape derivatives. The two computations being very similar, we will do this work for u_R only. To lighten the notations, we denote $u_\theta = u_R(\theta)$. We can notice that for every $\theta \in W_0^{1,\infty}(\mathcal{D})$, the functions u_θ are in $H_{\mathcal{O}_\theta}^1(\mathcal{D})$. To study the derivation of the application $\theta \mapsto u_\theta$, we consider the application $w(t) = u_\theta \circ (I + t\theta)$ defined on the space $H_{\mathcal{O}}^1(\mathcal{D})$, which does not depend on the choice of θ .

If u has a derivative \dot{u} , then we should have $\frac{w(t)-u}{t}$ that goes to \dot{u} . This remark gives us a candidate for the variational formulation that should be satisfied by \dot{u} . We will use that formulation to show that $\frac{w(t)-u}{t}$ effectively goes to \dot{u} and then compute the equation satisfied by the shape derivative u' thanks to the lemma 4.4.

By a change of variable $w(t)$ is solution of the weak problem

$$\int_{\mathcal{D}} (A(t)\nabla w \nabla \bar{v} - J(t)k^2 w \bar{v}) - ik_2 \int_{\partial\mathcal{D}} w \bar{v} = \int_{\partial\mathcal{D}} h \bar{v}, \quad \forall v \in V$$

where $J(t) = \det(I + tD\theta)$ and $A(t) = J(t)(I + tD\theta)^{-1}(I + tD\theta^T)^{-1}$. Subtracting by the variational form associated to u and dividing by $t \neq 0$, we get

$$\int_{\mathcal{D}} \left(A(t) \frac{\nabla w(t) - \nabla u}{t} \nabla \bar{v} - J(t)k^2 \frac{w(t) - u}{t} \bar{v} \right) - ik_2 \int_{\partial\mathcal{D}} \frac{w(t) - u}{t} \bar{v} = \int_{\mathcal{D}} \frac{I - A}{t} \nabla u \nabla \bar{v} - k^2 \frac{1 - J}{t} u \bar{v}, \quad \forall v \in V$$

The matrix A is usual in shape optimization and satisfies the following properties [1]: $A(t, x)$ is symmetric positive, $A(0) = I$ with

$$\mathcal{A} = \frac{d}{dt} A(t)|_{t=0} = \text{div}(\theta)I - (D\theta^T + D\theta)$$

and for t small enough, we have

$$\forall X \in \mathbb{R}^d, X^T A(t) X \geq \frac{\|X\|^2}{2}. \quad (4.2)$$

Similarly, the quotient $\frac{J(t)-1}{t}$ goes to $\text{div}(\theta)$ when t goes to 0 by differentiation of the \det application. Therefore, we let $\dot{u} \in V$ that satisfies

$$\int_{\mathcal{D}} (\nabla \dot{u} \nabla \bar{v} - k^2 \dot{u} \bar{v}) - ik_2 \int_{\partial\mathcal{D}} \dot{u} \bar{v} = - \int_{\mathcal{D}} \mathcal{A} \nabla u \nabla \bar{v} - k^2 \text{div}(\theta) u \bar{v}, \quad \forall v \in V$$

The function \dot{u} is well defined since this is the same variational form than the transmission problem, but with a different sesqui-linear term on the right. At this stage, we do not know if \dot{u} is the desired derivative. It is merely a candidate function that exists. Denote $\frac{w(t)-u}{t} - \dot{u}$ by $d(t)$. We are done if we show that $d(t)$ goes to 0 in $H^1(\mathcal{D})$. Subtracting the two last equations, we get

$$\begin{aligned} \int_{\mathcal{D}} A(t) \nabla d(t) \nabla \bar{v} - k^2 J(t) d(t) \bar{v} - ik_2 \int_{\partial\mathcal{D}} d(t) \bar{v} &= \int_{\mathcal{D}} \left[\left(\frac{I - A(t)}{t} + \mathcal{A} \right) \nabla u + (I - A(t)) \dot{u} \right] \nabla \bar{v} \\ &\quad - \int_{\mathcal{D}} k^2 \left[\left(\frac{1 - J(t)}{t} + \text{div}(\theta) \right) u + (1 - J(t)) \dot{u} \right] \bar{v}. \end{aligned}$$

We use $d(t)$ as a test function and proceed as in the last proof, by majoring the imaginary part of the left side by the modulus of the right side. Thus, using similar method than in the sub-section 4.1, we get by the Cauchy-Schwarz inequality and the continuity of J , for t small enough,

$$\|d(t)\|_{L^2(\partial\mathcal{D})}^2 \lesssim_{u,k,\dot{u}} \left(\left| \frac{I - A(t)}{t} + \mathcal{A} \right|_\infty + |I - A(t)|_\infty + \left| \frac{1 - J(t)}{t} + \text{div}(\theta) \right| + |1 - J(t)| \right) \|d(t)\|_{H^1(\mathcal{D})}$$

and

$$\|d(t)\|_{L^2(\mathcal{D})}^2 \lesssim_{u,k,\dot{u}} \left(\left| \frac{I - A(t)}{t} + \mathcal{A} \right|_\infty + |I - A(t)|_\infty + \left| \frac{1 - J(t)}{t} + \text{div}(\theta) \right| + |1 - J(t)| \right) \|d(t)\|_{H^1(\mathcal{D})},$$

where $\lesssim_{A,B}$ denotes being less than or equal to, up to a multiplicative constant that depends only on the quantities A and B .

Finally, if we come back to the whole expression with $d(t)$ as a test function, by the property (4.2) of A , we get

$$\|d(t)\|_{H^1(\mathcal{D})}^2 \lesssim_{u,k,\dot{u}} \left(\left| \frac{I - A(t)}{t} + \mathcal{A} \right|_\infty + |I - A(t)|_\infty + \left| \frac{1 - J(t)}{t} + \operatorname{div}(\theta) \right| + |1 - J(t)| \right) \|d(t)\|_{H^1(\mathcal{D})}$$

so that $\|d(t)\|_{H^1(\mathcal{D})} \rightarrow 0$ when t goes to zero. We have just shown that \dot{u} is the derivative of u . Consider now the shape derivative $u' = \dot{u} - \nabla u \cdot \theta$ (given by the lemma 4.4 with $\psi(\theta) = (I + \theta)^{-1}$ and $g(\theta) = u_\theta \circ (I + \theta)$). Adapting the computation of the step 4 of the proof of [1, Theorem 3.8], we first conclude that

$$\int_{\mathcal{D}} \nabla(\dot{u} - \nabla u \cdot \theta) \nabla \bar{v} = \int_{\mathcal{D}} (\nabla u' \nabla \bar{v} + \mathcal{A} \nabla u \nabla \bar{v} - k^2 u (\theta \cdot \nabla \bar{v})) .$$

Using the variational formulation satisfied by \dot{u} , we get

$$\begin{aligned} \int_{\mathcal{D}} (\nabla u' \nabla \bar{v} - k^2 u' \bar{v}) - ik_2 \int_{\partial\mathcal{D}} u' \bar{v} &= \int_{\mathcal{D}} k^2 u (\theta \cdot \bar{v}) + [(\nabla u \cdot \theta) + k^2 (\operatorname{div}(\theta) u + (\nabla u \cdot \theta))] \bar{v} \\ &= \int_{\mathcal{D}} k^2 u (\theta \cdot \nabla \bar{v}) + k^2 \operatorname{div}(u \theta) \bar{v} \\ &= \int_{\mathcal{D}} k^2 \operatorname{div}(u \theta \bar{v}). \end{aligned}$$

By the Green formula on both \mathcal{O}_1 and \mathcal{O}_2 , we have

$$\int_{\mathcal{D}} (\nabla u' \nabla \bar{v} - k^2 u' \bar{v}) - ik_2 \int_{\partial\mathcal{D}} u' \bar{v} = \int_{\partial\mathcal{O}_2 \cap \mathcal{O}_1} k_2^2 u \bar{v} (\theta \cdot n) + \int_{\partial\mathcal{O}_1} k_1^2 u \bar{v} (\theta \cdot n) = \int_{\partial\mathcal{O}_1} (k_1^2 - k_2^2) u \bar{v} (\theta \cdot n).$$

We recognize the weak formulation of the problem $\mathcal{T}(\mathcal{O}_1)$. By the lemma 4.3 below, we conclude that shape derivative exists and has the desired expression. \square

Proof of the adjoint method: proposition 2.4. By an integrations by part and the equation satisfied by ρ we have:

$$\begin{aligned} \int_{\mathcal{O}_i} \nabla u'_D \cdot \nabla(\overline{u_D - u_R}) &= \int_{\mathcal{O}_i} -(u'_D \Delta(\overline{u_D - u_R}) + \int_{\partial(\mathcal{O}_i)} u'_D \partial_n(\overline{u_D - u_R})) \\ &= \int_{\mathcal{O}_i} -u'_D (\Delta \rho_D + k^2 \rho_D) + \int_{\partial(\mathcal{O}_i)} u'_D \partial_n(\overline{u_D - u_R}) \\ &= \int_{\partial(\mathcal{O}_i)} \partial_n u'_D \rho_D - \partial_n \rho_D u'_D + u'_D \partial_n(\overline{u_D - u_R}). \end{aligned}$$

Similarly,

$$\int_{\mathcal{O}_i} \nabla u'_R \cdot \nabla(\overline{u_D - u_R}) = \int_{\partial\mathcal{O}_i} \partial_n u'_R \rho_R + u'_R (\partial_n(\overline{u_D - u_R}) - \partial_n \rho_R).$$

On $\partial\mathcal{D}$, the integrals are null thanks to the adjoint equation. Hence, we just need to compute the quantities

$$\mathcal{I}_D = \int_{\partial\mathcal{O}_1} \partial_n u'_D \rho_D + u'_D (\partial_n(\overline{u_D - u_R}) - \partial_n \rho_D) + \int_{\partial\mathcal{O}_2 \cap \mathcal{O}_1} \partial_n u'_D \rho_D + u'_D (\partial_n(\overline{u_D - u_R}) - \partial_n \rho_D)$$

and

$$\mathcal{I}_R = \int_{\partial\mathcal{O}_1} \partial_n u'_R \rho_R + u'_R (\partial_n(\overline{u_D - u_R}) - \partial_n \rho_R) + \int_{\partial\mathcal{O}_2 \cap \mathcal{O}_1} \partial_n u'_R \rho_R + u'_R (\partial_n(\overline{u_D - u_R}) - \partial_n \rho_R).$$

By the jump conditions and the identity $[ab] = [a]\frac{b_1+b_2}{2} + [b]\frac{a_1+a_2}{2}$, we have

$$\mathcal{I}_D = \int_{\partial\mathcal{O}_1} (k_1^2 - k_2^2) u_D \rho_D (\theta \cdot n) \quad \text{and} \quad \mathcal{I}_R = \int_{\partial\mathcal{O}_1} (k_1^2 - k_2^2) u_R \rho_R (\theta \cdot n)$$

so that

$$D_{\mathcal{O}_1} \mathcal{K}(\mathcal{O}_1, k_1)(\theta) = \Re \left(\int_{\mathcal{D}} \nabla(u'_D - u'_R) \cdot \nabla \overline{(u_D - u_R)} \right) = \Re \left(\int_{\mathcal{O}_1} (k_1^2 - k_2^2) (u_D \rho_D - u_R \rho_R) (\theta \cdot n) \right). \quad \square$$

To study the derivative with respect to the wavenumber, we proceed in a similar way. First, we compute a preliminary expression of the derivative. Then, we introduce the adjoint variables ρ_D and ρ_R in order to prove the proposition 2.5.

Lemma 4.6 (Derivative with respect to k)

For every k_1 admissible, the derivative of the functional (2.1) with respect to k_1 exists and

$$\frac{\partial \mathcal{K}(\mathcal{O}_1, k_1)}{\partial k_1} = \int_{\mathcal{D}} \nabla(u_D - u_R) \cdot \nabla \overline{(u'_D - u'_R)}, \quad (4.3)$$

where u'_R and $u'_D \in H^1(\mathcal{D})$ are solution to

$$\left\{ \begin{array}{lcl} \Delta u'_R + k_2^2 u'_R & = & 0 & \text{in } \mathcal{O}_2 \\ \Delta u'_R + k_1^2 u'_R & = & -2k_1 u_R & \text{in } \mathcal{O}_1 \\ \partial_n u'_R - ik u'_R & = & 0 & \text{on } \partial\mathcal{D} \\ [\partial_n u'_R] = [u'_R] & = & 0 & \text{on } \partial\mathcal{O}_1, \end{array} \right. \quad \left\{ \begin{array}{lcl} \Delta u'_D + k^2 u'_D & = & 0 & \text{in } \mathcal{O}_2 \\ \Delta u'_D + k_2^2 u'_D & = & -2k_1 u_D & \text{in } \mathcal{O}_1 \\ \partial_n u'_D - ik u'_D & = & 0 & \text{on } \Gamma_c \\ u'_D & = & 0 & \text{on } \Gamma_m \\ [\partial_n u'_D] = [u'_D] & = & 0 & \text{on } \partial\mathcal{O}_1. \end{array} \right.$$

Contrary to the proof of proposition 4.5, we will use the implicit function theorem, that is more convenient in our case. As before, we will only consider the derivatives of $k_1 \mapsto u_R(k_1)$.

Proof. Let us fix an admissible wave-number k_1 and define the function

$$F : \begin{cases} \mathbb{C} \times H^1(\mathcal{D}) \rightarrow (H^1(\mathcal{D}))' \\ (k, u) \mapsto (v \mapsto \int_{\mathcal{D}} \nabla u \nabla \bar{v} - k^2 u \bar{v} - ik \int_{\partial\mathcal{D}} (u + h) \bar{v}). \end{cases}$$

The application F is C^1 and is chosen such that $F(k, u) = 0$ if and only if u is solution to the problem $(\mathcal{T}(\mathcal{O}_1))$. We have

$$\partial_u F(k, u_R(k))(u)v = \int_{\mathcal{D}} \nabla u \nabla \bar{v} - k^2 u \bar{v} - ik \int_{\partial\mathcal{D}} u \bar{v}.$$

This is an isomorphism from $H^1(\mathcal{D})$ to $(H^1(\mathcal{D}))'$ by well-posedness of the problem $(\mathcal{T}(\mathcal{O}_1))$. By the implicit function theorem, there exists $\tilde{u} : C^0(\mathcal{D}, \mathbb{C}) \rightarrow H^1(\mathcal{D})$ a C^1 function defined on a neighborhood of 0 such that $F(k, \tilde{u}(k)) = 0$. By well-posedness of the problem $(\mathcal{T}(\mathcal{O}_1))$, we have $\tilde{u}(\mathcal{O}_1, k) = u_R(k)$ and $k \mapsto u_R(k)$ is C^1 on a neighborhood of k_1 . Then, derivating the variational form, we see that $u'_R(k_1)$ satisfy

$$\int_{\mathcal{D}} \nabla u'_R \nabla \bar{v} - k^2 u'_R \bar{v} - ik_2 \int_{\partial\mathcal{D}} u'_R \bar{v} = \int_{\mathcal{O}_1} 2k_1 u_R \bar{v}, \quad \forall v \in V.$$

This shows that u'_R satisfy the desired problem. \square

The expression of the derivative presented in Lemma 2.5 is sufficient to compute a gradient efficiently. However, this approach requires us to compute u'_R and u'_D at each step. A more efficient alternative is to compute the gradient using the adjoints ρ_D and ρ_R which have already been calculated. Consequently, the only additional cost is integrating a function over the domain to obtain the gradient with respect to k .

Proof of 2.5. We decompose the derivative as

$$\frac{\partial \mathcal{K}(\mathcal{O}_1, k_1)}{\partial k_1} = \Re \left(\int_{\mathcal{D}} \nabla u'_D \cdot \nabla \overline{(u_D - u_R)} \right) - \Re \left(\int_{\mathcal{D}} \nabla u'_R \cdot \nabla \overline{(u_D - u_R)} \right).$$

By integration by parts and the equation satisfied by ρ we have:

$$\begin{aligned}
\int_{\mathcal{D}} \nabla u'_D \cdot \nabla (\overline{u_D - u_R}) &= \int_{\mathcal{D}} -(u'_D \Delta (\overline{u_D - u_R}) + \int_{\partial \mathcal{D}} u'_D \partial_n (\overline{u_D - u_R})) \\
&= \int_{\mathcal{D}} -u'_D (\Delta \rho_D + k^2 \rho_D) + \int_{\partial \mathcal{D}} u'_D \partial_n (\overline{u_D - u_R}) \\
&= -\int_{\mathcal{D}} \rho_D (\Delta u'_D + k^2 u'_D) + \int_{\partial \mathcal{D}} \partial_n u'_D \rho_D - \partial_n \rho_D u'_D + u'_D \partial_n (\overline{u_D - u_R}) \\
&= 2 \int_{\mathcal{O}_1} \rho_D u_D k_1 + \int_{\partial \mathcal{D}} \partial_n u'_D \rho_D - \partial_n \rho_D u'_D + u'_D \partial_n (\overline{u_D - u_R}).
\end{aligned}$$

Decomposing the boundary as $\partial \mathcal{D} = \overline{\Gamma_c \cup \Gamma_m}$, we study the integral on each of the three parts. On Γ_m , $u'_D = \rho_D = 0$ and the integral is zero. On Γ_c , we write

$$\partial_n u'_D \rho_D - \partial_n \rho_D u'_D + u'_D \partial_n (\overline{u_D - u_R}) = u'_D (\partial_n \rho_D - ik \rho_D - \partial_n \rho_D) + \partial_n u'_D \rho_D = \rho_D (\partial_n u'_D - ik u'_D) = 0$$

so that the integral is also 0. Finally, we get $\int_{\mathcal{D}} \nabla u'_D \cdot \nabla (\overline{u_D - u_R}) = 2 \int_{\mathcal{O}_1} \rho_D u_D k_1$. Let us consider now the second term. The first step is exactly the same and we get

$$\int_{\mathcal{D}} \nabla u'_R \cdot \nabla (\overline{u_D - u_R}) = 2 \int_{\mathcal{O}_1} \rho_R u_R k_1 + \int_{\partial \mathcal{D}} \partial_n u'_R \rho_R - \partial_n \rho_R u'_R + u'_R \partial_n (\overline{u_D - u_R}).$$

On $\partial \mathcal{D}$, the terms that we integrate become

$$\partial_n u'_R \rho_R - \partial_n \rho_R u'_R + u'_R \partial_n (\overline{u_D - u_R}) = u'_R (\partial_n \rho_R - ik \rho_R - \partial_n \rho_R) + \partial_n u'_R \rho_R = \rho_R (\partial_n u'_R - ik u'_R) = 0.$$

Finally, we get $\int_{\mathcal{D}} \nabla u'_R \cdot \nabla (\overline{u_D - u_R}) = 2 \int_{\mathcal{O}_1} \rho_R u_R k_1$. Combining the two terms together, and using the equation satisfied by the derivatives on \mathcal{O} , we find

$$\frac{\partial \mathcal{K}(\mathcal{O}_1, k_1)}{\partial k_1} = 2 \int_{\mathcal{O}_1} (\rho_D u_D - \rho_R u_R) k_1. \quad \square$$

4.4 Proofs for the case with uncertainties

Proof of the expression of the expected value of the functional: proposition 2.6. The computation is done through the Fubini theorem (all the quantities are L^2 and positive) after developing the term and arranging them to factor out the powers of Y . Indeed, let us keep in mind that $\mathbb{E}(Y_i) = 0$, $\mathbb{E}(Y_i Y_j) = \delta_{i,j}$, $\mathbb{E}(Y_i Y_j Y_k Y_l) = 1$ when the indices pair up and is equal to $\mathbb{E}(Y^4)$ if they are all equal. Otherwise, it is 0.

$$\begin{aligned}
\mathbb{E}(\mathcal{E}_{\mathcal{K}}(\mathcal{O}_1, k_1)) &= \frac{1}{2} \int_{\Omega} \int_{\mathcal{D}} \left| \sum_{m=0}^M (\nabla u_{R_m} - \nabla u_{D_m}) Y_m(\omega) \right|^2 dx d\mathbb{P}(\omega) \\
&= \int_{\Omega} \int_{\mathcal{D}} \left(\sum_{m=0}^M |\nabla u_{D_m} - \nabla u_{R_m}|^2 Y_m(\omega)^2 \right. \\
&\quad \left. + \sum_{0 \leq m \neq l \leq M} (\nabla u_{D_l} - \nabla u_{R_l}) \cdot \overline{(\nabla u_{D_m} - \nabla u_{R_m})} Y_l(\omega) Y_m(\omega) \right) dx d\mathbb{P}(\omega) \\
&= \frac{1}{2} \int_{\mathcal{D}} \sum_{m=0}^M |\nabla u_{D_m} - \nabla u_{R_m}|^2 dx. \quad \square
\end{aligned}$$

We recognize the sum of $M+1$ terms of the form $\int_{\mathcal{D}} |\nabla u_D - \nabla u_R|^2$. Using the results of the deterministic case (propositions 4.5 and 2.5), we deduce the desired formula.

Proof of the expression of the variance of the functional: proposition 2.7. We proceed in the same way as in the previous proof. The expression is more complex, but still entirely computable numerically.

$$\mathbb{E}(\mathcal{E}_K(\mathcal{O}, \omega)^2) = \frac{1}{4} \int_{\Omega} \left(\int_{\mathcal{D}} \left| \sum_{m=0}^M (\nabla u_{R_m} - \nabla u_{D_m}) Y_m(\omega) \right|^2 dx \right)^2 d\mathbb{P}(\omega).$$

We use Fubini's theorem and the particular case where $Y \sim \mathcal{N}(0, 1)$: we use $\mathbb{E}(Y_m) = 0$, $\mathbb{E}(Y_m^3) = 0$, $\mathbb{E}(Y_m^4) = 3$.

$$\begin{aligned} \mathbb{E}(\mathcal{E}_K(\mathcal{O}, \omega)^2) &= \frac{1}{4} \int_{\Omega} \left(\int_{\mathcal{D}} |\nabla d_0|^2 + 2\Re \left(\nabla d_0 \cdot \sum_{m=1}^M \overline{\nabla d_m} Y_m \right) + \left| \sum_{m=1}^M \nabla d_m Y_m \right|^2 \right)^2 \\ &= \frac{1}{4} \left(\int_{\mathcal{D}} |\nabla d_0|^2 \right)^2 + \frac{1}{2} \left(\int_{\mathcal{D}} |\nabla d_0|^2 \right) \int_{\Omega} \left(\int_{\mathcal{D}} \left| \sum_{m=1}^M \nabla d_m Y_m \right|^2 \right) \\ &\quad + \int_{\Omega} \left(\int_{\mathcal{D}} \Re \left(\nabla d_0 \cdot \sum_{m=1}^M \overline{\nabla d_m} Y_m \right) \right)^2 + \frac{1}{4} \int_{\Omega} \left(\int_{\mathcal{D}} \left| \sum_{m=1}^M \nabla d_m Y_m \right|^2 \right)^2 \\ &= \frac{1}{4} \left(\int_{\mathcal{D}} |\nabla d_0|^2 \right)^2 + \frac{1}{2} \left(\int_{\mathcal{D}} |\nabla d_0|^2 \right) \left(\sum_{m=1}^M \int_{\mathcal{D}} |\nabla d_m|^2 \right) \\ &\quad + \sum_{m=1}^M \left(\int_{\mathcal{D}} \Re \left(\nabla d_0 \cdot \nabla \overline{d_m} \right) \right)^2 + \Re \left(\sum_{1 \leq m < l \leq M} \left(\int_{\mathcal{D}} \nabla d_m \overline{\nabla d_l} \right)^2 \right) \\ &\quad + \frac{3}{4} \sum_{m=1}^M \left(\int_{\mathcal{D}} |\nabla d_m|^2 \right)^2 + \frac{1}{2} \sum_{1 \leq m < l \leq M} \left(\int_{\mathcal{D}} |\nabla d_m|^2 \right) \left(\int_{\mathcal{D}} |\nabla d_l|^2 \right) \end{aligned}$$

With the same notations, we have

$$\mathcal{E}_K(\mathcal{O}_1, k_1)^2 = \frac{1}{4} \left(\sum_{m=0}^M \int_{\mathcal{D}} |\nabla d_m|^2 \right)^2 = \frac{1}{4} \sum_{m=0}^M \left(\int_{\mathcal{D}} |\nabla d_m|^2 \right)^2 + \frac{1}{2} \sum_{1 \leq m < l \leq M} \left(\int_{\mathcal{D}} |\nabla d_m|^2 \right) \left(\int_{\mathcal{D}} |\nabla d_l|^2 \right).$$

Thus,

$$\begin{aligned} \mathbb{V}(\mathcal{E}_K(\mathcal{O}, \omega)) &= \frac{1}{4} \left(\int_{\mathcal{D}} |\nabla d_0|^2 \right)^2 + \frac{1}{2} \left(\int_{\mathcal{D}} |\nabla d_0|^2 \right) \left(\sum_{m=1}^M \int_{\mathcal{D}} |\nabla d_m|^2 \right) \\ &\quad + \sum_{m=1}^M \left(\int_{\mathcal{D}} \Re \left(\nabla d_0 \cdot \nabla \overline{d_m} \right) \right)^2 + \Re \left(\sum_{1 \leq m < l \leq M} \left(\int_{\mathcal{D}} \nabla d_m \overline{\nabla d_l} \right)^2 \right) \\ &\quad + \frac{1}{2} \sum_{m=1}^M \left(\int_{\mathcal{D}} |\nabla d_m|^2 \right)^2 \end{aligned}$$

First, we denote u'_{D_i} and u'_{R_i} the derivatives of the function $\mathcal{O}_1 \mapsto u_{D_i}(\mathcal{O}_1)$ and $\mathcal{O}_1 \mapsto u_{R_i}(\mathcal{O}_1)$ as computed in the deterministic case. The expression becomes

$$\begin{aligned}
D_{\mathcal{O}_1} \mathbb{V}((\mathcal{O}_1, k_1))(\theta) = & \frac{1}{2} \left(\int_{\mathcal{D}} |\nabla d_0|^2 \right) D_{\mathcal{O}_1} \mathcal{E}_{\mathcal{K}}(\mathcal{O}_1, k_1)(\theta) + 2 \sum_{m=1}^M \left(\int_{\mathcal{D}} \Re (\nabla d_0 \cdot \nabla \overline{d_m}) \right) \left(\int_{\mathcal{D}} \Re (\nabla d_0 \cdot \nabla \overline{d'_m}) \right) \\
& + 2 \sum_{1 \leq m < l \leq M} \Re \left(\int_{\mathcal{D}} \nabla d_m \overline{\nabla d_l} \right) \Re \left(\int_{\mathcal{D}} \nabla d_m \overline{\nabla d'_l} + \nabla d'_m \overline{\nabla d_l} \right) \\
& + \sum_{m=1}^M \left(\int_{\mathcal{D}} |\nabla d_m|^2 \right) \Re \left(\int_{\partial \mathcal{O}_1} (k_1^2 - k_2^2) p_{m,m}(\theta \cdot n) \right).
\end{aligned}$$

Finally, the expression takes the form

$$D_{\mathcal{O}_1} \mathbb{V}((\mathcal{O}_1, k_1))(\theta) = \Re \left(\int_{\partial \mathcal{O}_1} (k_1^2 - k_2^2) \mathcal{G}(\theta \cdot n) \right),$$

where

$$\begin{aligned}
\mathcal{G} = & \frac{1}{2} \left(\int_{\mathcal{D}} |\nabla d_0|^2 \right) \sum_{m=1}^M p_{m,m} + 2 \sum_{m=1}^M \left(\int_{\mathcal{D}} \Re (\nabla d_0 \cdot \nabla \overline{d_m}) \right) p_{0,m} \\
& + 4 \sum_{1 \leq m < l \leq M} \Re \left(\int_{\mathcal{D}} \nabla d_m \overline{\nabla d_l} \right) p_{m,l} + \sum_{m=1}^M \left(\int_{\mathcal{D}} |\nabla d_m|^2 \right) p_{m,m}.
\end{aligned}$$

We proceed in the same way to derivate with respect to the wavenumber k . \square

Acknowledgement. F. Caubet was funded by the ANR project STOIQUES (ANR-24-CE40-2216) and the PHC TOUBKAL project 51628SC.

References

- [1] L. Afraites, M. Dambrine, K. Eppler, and D. Kateb. Detecting perfectly insulated obstacles by shape optimization techniques of order two. *Discrete and Continuous Dynamical Systems - B*, 8(2):389–416, 2007.
- [2] G. Allaire. *Conception optimale de structures*, volume 58 of *Mathématiques & Applications*. Springer, Paris, 2007.
- [3] L. Audibert, H. Haddar, and X. Liu. An accelerated level-set method for inverse scattering problems. *SIAM Journal on Imaging Sciences*, 15(3):1576–1600, 2022.
- [4] T. Bonnafont and F. Caubet. Inverse scattering using a kohn-vogelius formulation and shape optimization method. In *2023 17th European Conference on Antennas and Propagation (EuCAP)*, pages 1–5. IEEE, 2023.
- [5] L. Bourgeois, N. Chaulet, and H. Haddar. On simultaneous identification of the shape and generalized impedance boundary condition in obstacle scattering. *SIAM Journal on Scientific Computing*, 34(3):A1824–A1848, 2012.
- [6] K. E.-G. Boutarene, S. Galleze, and V. Péron. On Ventcel-type transmission conditions for a Helmholtz problem with a non-uniform thin layer. *SeMA Journal: Boletín de la Sociedad Española de Matemática Aplicada*, 2024.
- [7] O. Bucci and T. Isernia. Electromagnetic inverse scattering: Retrievable information and measurement strategies. *Radio science*, 32(6):2123–2137, 1997.

- [8] F. Cakoni, D. Colton, and H. Haddar. *Inverse scattering theory and transmission eigenvalues*. SIAM, 2022.
- [9] F. Cakoni, D. Colton, and P. Monk. *The linear sampling method in inverse electromagnetic scattering*. SIAM, 2011.
- [10] F. Cakoni and D. L. Colton. *A qualitative approach to inverse scattering theory*, volume 767. Springer, 2014.
- [11] F. Caubet, M. Dambrine, D. Kateb, and C. Z. Timimoun. A Kohn-Vogelius formulation to detect an obstacle immersed in a fluid. *Inverse Problems and Imaging*, 7(1):123–157, 2013.
- [12] S. Chaabane, H. Haddar, and R. Jerbi. A combination of Kohn-Vogelius and DDM methods for a geometrical inverse problem. *Inverse Problems*, 39(9):095001, July 2023.
- [13] D. Colton and R. Kress. *Integral Equation Methods in Scattering Theory*. Society for Industrial and Applied Mathematics, Philadelphia, PA, 2013.
- [14] D. Colton and R. Kress. *Inverse Acoustic and Electromagnetic Scattering Theory*, volume 93 of *Applied Mathematical Sciences*. Springer, New York, 4 edition, 2019.
- [15] L. Crocco, I. Catapano, L. Di Donato, and T. Isernia. The linear sampling method as a way to quantitative inverse scattering. *IEEE Transactions on Antennas and Propagation*, 60(4):1844–1853, 2012.
- [16] M. Dambrine and V. Karnaev. Robust obstacle reconstruction in an elastic medium. *Discrete and Continuous Dynamical Systems - Series B*, 29(1):151–173, 2024.
- [17] J. Dardé. *Méthodes de quasi-réversibilité et de lignes de niveau appliquées aux problèmes inverses elliptiques*. Theses, Université Paris-Diderot - Paris VII, Dec. 2010.
- [18] J. Dardé, N. Hyvönen, A. Seppänen, and S. Staboulis. Simultaneous recovery of admittivity and body shape in electrical impedance tomography: an experimental evaluation. *Inverse Problems*, 29(8):085004, 16, 2013.
- [19] O. Dorn, E. L. Miller, and C. M. Rappaport. A shape reconstruction method for electromagnetic tomography using adjoint fields and level sets. *Inverse Problems*, 16(5):1119, oct 2000.
- [20] A. Ern and J.-L. Guermond. *Finite Elements II: Galerkin Approximation, Elliptic and Mixed PDEs*. Springer, 2021.
- [21] B. Faverjon, B. Puig, and T. Baranger. Identification of boundary conditions by solving cauchy problem in linear elasticity with material uncertainties. *Computers & Mathematics with Applications*, 73(3):494–504, 2017.
- [22] F. Feppon. *Shape and topology optimization of multiphysics systems*. PhD thesis, Thèse de doctorat de l’Université Paris-Saclay préparée à l’école polytechnique, 2019.
- [23] F. Hecht. New development in freefem++. *J. Numer. Math.*, 20(3-4):251–265, 2012.
- [24] A. Henrot and M. Pierre. *Shape Variation and Optimization*, volume 28 of *EMS Tracts in Mathematics*. European Mathematical Society, Zürich, 2018.
- [25] R. Kress. Inverse scattering from an impedance boundary condition. *Mathematical Methods in the Applied Sciences*, 41(16):6343–6354, 2018.
- [26] A. Litman, D. Lesselier, and F. Santosa. Reconstruction of a two-dimensional binary obstacle by controlled evolution of a level-set. *Inverse Problems*, 14(3):685, jun 1998.
- [27] Nesterov and Y. E. A method for solving the convex programming problem with convergence rate $O(1/k^2)$. *Dokl. Akad. Nauk SSSR*, 269(3):543–547, 1983.

- [28] O'Donoghue, Brendan, and E. Candès. Adaptive restart for accelerated gradient schemes. *Found. Comput. Math.*, 15(3):715–732, 2015.
- [29] Y. Wen, N. de Beaucoudrey, J. Chauveau, and P. Pouliquen. Algorithm for profile function calculation of 3d objects: application for radar target identification in low frequency. *Progress In Electromagnetics Research B*, 50:273–293, 2013.